Atmos. Chem. Phys. Discuss., 3, 1973–1989, 2003
www.atmos-chem-phys.org/acpd/3/1973/

Atmospheric Chemistry and Physics Discussions

Improving the seasonal cycle and interannual variations of biomass burning aerosol sources

S. Generoso[1], F.-M. Bréon[1], Y. Balkanski[1], O. Boucher[2], and M. Schulz[1]

[1]Laboratoire des Sciences du Climat et de l'Environnement, CEA/CNRS, Gif-sur-Yvette, France
[2]Laboratoire d'Optique Atmosphérique, CNRS/Université des Sciences et Technologies de Lille, Villeneuve d'Ascq, France

Received: 31 January 2003 – Accepted: 24 March 2003 – Published: 15 April 2003

Correspondence to: S. Generoso (generoso@lsce.saclay.cea.fr)

Abstract

This paper suggests a method for improving current inventories of aerosol emissions from biomass burning. The method is based on the hypothesis that, although the total estimates within large regions are correct, the exact spatial and temporal description can be improved. It makes use of open fire detection from the ATSR instrument that is available for a period of 5 years starting in 1996. Thus, the emissions inventories are re-distributed in space and time according to the occurrence of open fires.

The impact of the method on the emission inventories is assessed using an aerosol transport model, the results of which are compared to sunphotometer and satellite data. It is shown that the seasonal cycle of aerosol load in the atmosphere is significantly improved in several regions, in particular South America and Australia. Besides, the use of ATSR fire detection may be used to account for interannual events, as is demonstrated on the large Indonesian fires of 1997, a consequence of the 1997–1998 El Niño. Despite these improvements, there are still some large discrepancies between the simulated and observed optical thicknesses.

1. Introduction

Aerosols affect the Earth radiative balance through diverse processes (direct and indirect effects), which are qualitatively well understood (Charlson et al., 1992; Twomey, 1977) but quantitatively still poorly known (Haywood and Boucher, 2000; IPCC, 2001). There are many evidence of a large effect of aerosols on climate both at regional (Léon et al., 2002) and global (Bréon et al., 2002) scale. Improving our knowledge requires, in particular, a better representation of aerosols in atmospheric models, which requires, among others, an accurate representation of sources (see Fig. 4 of Charlson et al., 1992). In this paper, we focus on biomass burning, which is the main source of carbonaceous aerosols (Black Carbon (BC) and Organic Carbon (OC)). The two emission inventories most often used in general circulation models (GCM) are that of Liousse

ACPD

3, 1973–1989, 2003

et al. (1996) and GEIA (Global Emissions Inventory Activity, a part of the International Global Atmospheric Chemistry (IGAC) Project). Although satellite data have been used to describe the monthly distribution of emissions over Africa (Cooke et al., 1996), the seasonal cycles are not well represented in many regions and interannual variations are not accounted for. Satellites are well suited to provide such information because of their global and continuous coverage. This study describes a method that generates emission maps of biomass burning aerosol, which couples the inventories (Lavoué et al., 2000; Liousse et al., 1996) to the occurrence of fires as detected by ATSR-2 (Along Track Scanning Radiometer). This work has some similarities with that of Schultz (2002) but shows in addition a comparison with satellite and ground based measurements. The method presented in Duncan et al. (2003) is similar but applied to carbon monoxide emissions.

2. Method

The monthly emission maps have been created as follow. First, the globe is divided into boxes that contain fairly homogeneous vegetation cover and fire season. In high latitude regions, the boxes follow the work of Lavoué et al. (2000), based on state borders and dominant vegetation (blue boxes in Fig. 1). Within each box, we compute the total annual emission according to the inventories.

Similarly, we compute within each box the total number of fires detected by the ATSR instrument during the period (July 1997–May 1997) U (June 1998–December 2001). The period from June 1997 to May 1998 was omitted since it is strongly affected by an El Niño event, which resulted in very abnormal fire activity. We also removed from the datasets the "hot-spots" occurring in the same place during several months, as those are likely to be a result of industrial flares. The Hot Spots, likely to be agricultural or wild fires, are detected based on a simple 317 K threshold on the 3.7 μm channel on night-time observations (Arino and Melinotte, 1995). This product appears well suited for our needs as it is sensitive to fires that are small compared to the 1x1 km2

ACPD
3, 1973–1989, 2003

pixel, and because there is no orbit drift on the platform, which makes possible year-to-year comparisons. On the other hand, it suffers from well-known drawbacks that are discussed in the next section. A cloud coverage correction was applied by weighting the number of fires by $(1\text{-}C)^{-1}$ where C is the monthly climatological cloud cover (New et al., 1999), which assumes that occurrences of clouds and fires are not correlated.

From these two datasets, we compute for each box the ratio between the annual emitted quantities of carbonaceous aerosols (Q) and the annual mean number of detected fires after having applied the cloud cover correction (N). This Emission Constant (EC) is a statistical estimate of the emitted mass per detected fire. It varies depending on the box but is assumed constant within a given box, all through the year and from one year to the next.

Using EC and the monthly Hot-Spot distributions at the chosen resolution, we compute an emission estimate for all months when ATSR data is available (July 1996 to January 2002 at the time of the study). In the results presented in the following, the resolution was chosen in agreement with the atmospheric model resolution ($3.75\times2.5^{\circ}$ in longitude and latitude, respectively) although the same procedure would apply to finer grids. Note that the inventory emissions are redistributed as a function of time, but also within the boxes of Fig. 1 (the annual inventory emissions are aggregated at the scale of the boxes and re-distributed within, according to the locations of the Hot Spots). In order to provide an emission estimate for the periods when no ATSR data is available, we also computed a "climatological" monthly emission based on the mean number of fires observed during a given month for the same period that excludes El Niño.

3. Discussion

This method provides a simple way to introduce a seasonal cycle and interannual variations of biomass burning in the inventories. On the other hand, it requires unproven assumptions. A first assumption stems from the use of night observations only. As

ACPD
3, 1973–1989, 2003

a consequence, the emission distribution is only based on fires that extend into the night. This hypothesis does not impact the mean emissions in a box as it is implicitly accounted for in the Emission Constant EC. On the other hand, the method will fail if the ratio between the number of day-time and night-time fires varies significantly, within a box, between months or between the various pixels of the emission grid.

Cloud coverage is also a source of uncertainty as it prevents the detection of surface fires. We have attempted to correct for the cloud coverage using a monthly climatology. Nevertheless significant uncertainty remain as the cloud cover may differ from the climatology (in particular during specific meteorological events) and also because the night- time mean cloud cover may differ from the daily climatology.

Another potential problem results from the satellite coverage that increases with latitude (a high latitude point is sampled more frequently than a low latitude one), augmenting the probability of fire detection. On the other hand, the boxes of Fig. 1 are small enough so that the satellite revisit frequency does not change significantly within a box. As our method computes EC box by box, the variation of satellite coverage with the latitude is implicitly accounted for.

Finally, these maps have been made assuming that in each box, the emission efficiency of fires for BC or OC has no seasonal or interannual variation (EC is constant). This is a rather strong assumption as, for a given vegetation type, the emitted quantities depend on several parameters such as ground humidity, vegetation state or burns history, that vary with the season.

4. Results and validation

The new emission maps have been used as input of the Laboratoire de Météorologie Dynamique (LMD) General Circulation Model, LMDz, coupled with INCA (Interaction with Chemistry and Aerosols) which is an emission/chemistry model (http://www.ipsl.jussieu.fr/~dhaer/inca/). We use the model with a resolution of 96×72 (3.75×2.5° in longitude and latitude) and 19 hybrid vertical levels. Only carbonaceous aerosols were

ACPD
3, 1973–1989, 2003

analyzed in this study. The model can include its own dynamics, although we nudged here the meteorological fields from the 6-h ECMWF reanalysis. It generates fields of aerosol load ($g.m^{-2}$) that are converted into optical thicknesses at 865 nm using constant factors ($3.5\,m^2.g^{-1}$ for OC and $4.5\,m^2.g^{-1}$ for BC, Dubovik et al., 2002; Liousse et al., 1995; Liousse et al., 1996) based on typical size distributions of biomass burning aerosols.

4.1. Seasonal cycle

Ground-based measurements from different AERONET (Holben et al., 1998) sites in South America, Africa and Australia are used to validate our simulations. Comparisons are also made with satellite observations from the POLDER (POLarization and Directionality of the Earth Reflectances, Deschamps et al., 1994) spaceborne instrument, which is well suited to study aerosols and in particular biomass burning aerosols. The Aerosol Index from POLDER (Deuzé et al., 2001), available both over land and ocean, is an indicator of submicronic aerosol load only, thus mainly sulfate, BC and OC. The analysis of POLDER retrievals (Tanré et al., 2001) provides a rough identification of the aerosol origin.

In a first step, we discuss the results over South America, as it is a major region of biomass burning activity. Alta Floresta (9° S, 56° W) and Abracos Hill (10° S, 62° W) are selected because long-time series of data are available. Figure 2 shows the mean AERONET Aerosol Optical Thickness at 870 nm (AOT_{870}) (in blue), the simulation results using the new sources (red) and those using the previous sources from Liousse et al. (1996) (in green). AERONET data show the impact of the biomass burning activity from August to November with a maximum value generally in September during three consecutive years from 1999 to 2001. The model results indicate that seasonal cycle is better depicted with the corrected emission maps, beginning at least two months later than the original sources, in agreement with the observed aerosol loads. On the other hand, the simulated results decrease rapidly after September, whereas the observations indicate the presence of significant load extending up to October. The AERONET

measurements at Abracos Hill for the year 2000 show a significant anomaly that is not depicted by our simulations. ATSR fire counts do not show particularly large numbers during that year. At present, we do not have a satisfactory explanation for this discrepancy between the measurements and the simulated optical thicknesses.

Over Australia, Jabiru (12° S, 132° E) is the only site in the North with sufficient amount of data. Although the seasonal cycle is not complete, the maximum aerosol load appears to be in September and October. The corrected emission maps lead to a clear improvement of the seasonal cycle although the magnitude of the optical depth is somewhat too small.

Over the African continent there are two main areas of biomass burning. One extends along 10° of latitude with the main activity between November and February. The other large burning area of Africa extends over the southern subtropics, with an activity that starts in June in the western part of the area, moves to the East and Madagascar, and ends in November. Figure 2 shows the comparison results over Ilorin (8° N, 4° E), Mongu (15° S, 23° E) and Skukuza (24° S, 31° E) sites, which were chosen for their extended time series. These comparisons indicate that the original emission maps show a satisfactory seasonal cycle that is not improved nor degraded using the information from the ATSR. On the other hand, the modeled optical thicknesses are much smaller than the observations, which can be a result of an underestimate of the emission fluxes, although the factor used to convert masses to optical thicknesses can also be blamed.

In order to have a global view of the representation of carbonaceous aerosols in the model, we show on Figs. 3a and 3b a comparison between POLDER AI (a good index for carbonaceous and sulfate aerosols) and LMDZ AI. The simulation overlaps the period of the POLDER data, i.e. from October 1996 to September 1997. For consistency with the satellite measurements, the model simulates the source and cycle of carbonaceous and sulfate (Boucher et al., 2002) aerosols. The global picture confirms several findings of the AERONET comparisons. Figure 3a shows that both inventories depict correctly the phase of the aerosol load seasonal cycle in Western Africa. It is also noteworthy that the model under predicts the aerosol index from November to

ACPD
3, 1973–1989, 2003

March. The satellite data confirm that there is no significant aerosol load over South America from May to June (see middle panel on Fig. 3b). The model predictions using the ATSR-derived inventory are in agreement with observations, contrary to what the model predicts with the original sources in May and June. The use of information from ATSR fires brings about an even larger change in the phasing of biomass burning over North Australia. The original sources yield a significant aerosol load from May to September, when the corrected sources indicate that the fire activity starts in September.

4.2. Interannual events

In order to show that the proposed method accounts for large interannual variations, we focus on the particular event of Indonesian fires that took place in September/October 1997 (Nakajima et al., 1999), thought to be a consequence of 1997/1998 El Niño. This phenomenon was well captured by the Earth-Probe TOMS (Herman et al., 1997). Figure 4 shows a comparison between TOMS AI and LMDZ AOT_{865} based upon the Liousse et al. (1996) inventory and upon the ATSR-derived inventory. Note that although an exact quantitative comparison is difficult, the emissions from these fires are reproduced qualitatively through the use of ATSR fire counts. TOMS measurements indicate a large aerosol load over Indonesia in September and October 1997. The consequence of the abnormal fire activity is not depicted with the original inventory, as one would expect for a climatological source. By contrast, the use of ATSR-based emission maps leads to an aerosol index significantly larger than for other years (i.e. October 1998 in Fig. 4). In the emission maps, the location of the emitted quantities are consistent with TOMS observations (not shown) although Fig. 4 suggests that BC and OC column burdens are underestimated. The gradients in optical depths away from sources derived by TOMS are not well reproduced by the simulation, which points to a model shortcoming. At present, the model does not account for the change in hydrophilic behavior of carbonaceous aerosol as it ages. This feature, which could

ACPD
3, 1973–1989, 2003

impact strongly the aerosol distribution, is currently being added to the model.

5. Conclusions

The method described in this paper provides a simple way to introduce fire seasonal cycles into already existing inventories and to take into account interannual variations. The comparison of the aerosol transport simulations to in-situ and satellite measurements clearly show an improvement when using the fire count information. In particular, the aerosol load seasonal cycle over South America and Australia, which are not well represented in the original inventories, are now better depicted. The comparison with POLDER products provides a global and qualitative validation of the seasonal cycle of biomass burning aerosol. Due to the rather short observing period of POLDER-1, the analysis of the seasonal cycle is incomplete, and we are expecting additional information from the recently launched POLDER-2 instrument onboard ADEOS-II. The comparison of the model simulations with AERONET data allows more quantitative comparison over specific sites. These comparisons confirm the improvement when using the fire count data to constrain the seasonal cycle and the inter-annual events, although significant discrepancies were found in the amplitude of the aerosol load in particular toward the end of the biomass burning season.

The European Space Agency (ESA) has recently made available new ATSR products that quantify the burned surfaces (GLOBSCAR, http://shark1.esrin.esa.it/ionia/FIRE/BS/ATSR/). This dataset may provide another, more precise opportunity to scale the emissions and their seasonal cycle, although only the year 2000 is yet available.

Acknowledgement. The emission factors are based on the ATSR World Fire Atlas managed by the European Space Agency (ESA). We thank C. Liousse for providing the OC and BC emission inventories. We thank the principal investigators B. Holben, P. Artaxo, R. Mitchell and R. Pinker and the AERONET program team for providing the ground-based aerosol data used in this work. The satellite data come from the POLDER instrument developed by the Centre National d'Etudes Spatiales onboard the ADEOS platform developed by NASDA.

References

Arino, O. and Melinotte, J. M.: Fire index atlas, Earth observation quaterly, 50, 1995.

Boucher, O., Pham, M., and Venkataraman, C.: Simulation of the atmospheric sulfur cycle in the Laboratoire de Météorologie Dynamique General Circulation Model. Model description, model evaluation, and global and European budgets, Notes scientifiques de l'IPSL, (available at http://www.ipsl.jussieu.fr/poles/Modelisation/NotesSciences.htm), 2002.

Bréon, F.-M., Tanré, D., and Generoso, S.: Aerosol effect on cloud droplet size monitored from satellite, Science, 295, 834–838, 2002.

Charlson, R. J., Schwartz, S. E., Hales, J. M., Cess, R. D., Coakley, J. A. J., Hansen, J. E., and Hofmann, D. J.: Climate forcing by anthropogenic aerosols, Science, 255, 423–430, 1992.

Chiapello, I., Goloub, P., Tanré, D., Marchand, A., Herman, J., and Torres, O.: Aerosol detection by TOMS and POLDER over oceanic regions, Journal of Geophysical Research – Atmospheres, 105, 7133–7142, 2000.

Cooke, W. F., Koffi, B., and Grégoire, J.-M.: Seasonality of vegetation fires in Africa from remote sensing data and application to a global chemistry model, Journal of Geophysical Research – Atmospheres, 101, 21 051–21 065, 1996.

Deschamps, P.-Y., Bréon, F.-M., Leroy, M., Podaire, A., Bricaud, A., Buriez, J.-C., and Sèze, G.: The POLDER mission: instrument characteristics and scientific objectives, IEEE Transactions on geoscience and remote sensing, 32, 598–615, 1994.

Deuzé, J. L., Bréon, F.-M., Devaux, C., Goloub, P., Herman, M., Lafrance, B., Maignan, F., Marchand, A., Nadal, F., Perry, G., and Tanré, D.: Remote sensing of aerosols over land surfaces from POLDER-ADEOS-1 polarized measurements, Journal of Geophysical Research, 106, 4913–4926, 2001.

Dubovik, O., Holben, B., Eck, T. F., Smirnov, A., Kaufman, Y. J., King, M. D., Tanré, D., and Slutsker, I.: Variability of absorption and optical properties of key aerosol types observed in worldwide locations, Journal of the Atmospheric Sciences, 59, 590–608, 2002.

Duncan, B. N., Randall, V. M., Staudt, A. C., Yevich, R., and logan, J. A.: Interannual and seasonal variability of biomass burning emissions constrained by satellite observations, Journal of Geophysical Research – Atmospheres, 108, 4040, doi:10.129/2002JD002378, 2003.

Haywood, J. and Boucher, O.: Estimates of the direct and indirect radiative forcing due to tropospheric aerosols: a review, Reviews of Geophysics, 38, 513–543, 2000.

Herman, J. R., Bhartia, P. K., Torres, O., Hsu, C., Seftor, C., and Celarier, E.: Global distribution

of UV-absorbing aerosols from Nimbus 7/TOMS data, Journal of Geophysical Research - Atmospheres, 102, 16 911–16 922, 1997.

Holben, B. N., Eck, T. F., Slutsker, I., Tanré, D., Buis, J. P., Setzer, A., Vermote, E., Reagan, J. A., Kaufman, Y. J., Nakajima, T., Lavenu, F., Jankowiak, I. and Smirnov, A.: AERONET – A federated intrument network and data archive for aerosol characterization, Remote Sensing of Environment, 66, 1–16, 1998.

IPCC: Climate change 2001: The scientific basis, contribution of working group I to the third assessment. Report of the Intergovernmental Panel on Climate Change, Cambridge University Press, New York, USA, 881, 2001.

Lavoué, D., Liousse, C., Cachier, H., Stocks, B. J., and Goldammer, J. G.: Modeling of carbonaceous particles emitted by boreal and temperate wildfires at northern latitudes, Journal of Geophysical Research – Atmospheres, 105, 26 871–26 890, 2000.

Léon, J.-F., Chazette, P., Pelon, J., Dulac, F., and Randriamiarisoa, H.: Aerosol direct radiative impact over the INDOEX area based on passive and active remote sensing, Journal of Geophysical Research – Atmospheres, 107, 10129, doi:10.1029/2000JD000116, 2002.

Liousse, C., Devaux, C., Dulac, F., and Cachier, H.: Aging of savanna biomass burning aerosols: consequences on their optical properties, Journal of Atmospheric Chemistry, 22, 1–17, 1995.

Liousse, C., Penner, J. E., Chuang, C., Walton, J. J., Eddleman, H., and Cachier, H.: A global three-dimensional model study of carbonaceous aerosols, Journal of Geophysical Research – Atmospheres, 101, 19 411–19 432, 1996.

Nakajima, T., Higurashi, A., Takeuchi, N., and Herman, J. R.: Satellite and ground-based study of optical properties of 1997 Indonesian forest fire aerosols, Geophysical Research Letters, 26, 2421–2424, 1999.

New, M., Hulme, M., and Jones, P.: Representing twentieth-century space-time climate variability. Part I: Development of a 1961–1990 mean monthly terrestrial climatology, Journal of Climate, 12, 829–856, 1999.

Schultz, M. G.: On the use of ATSR fire count data to estimate the seasonal and interannual variability of vegetation fire emissions, Atmospheric Chemistry and Physics, 2, 387–395, 2002.

Tanré, D., Bréon, F.-M., Deuzé, J.L., Herman, M., Goloub, P., Nadal, F., and Marchand, A.: Global observation of anthropogenic aerosols from satellite, Geophysical Research Letters, 28, 4555–4558, 2001.

Twomey, S.: The influence of pollution on the shortwave albedo of clouds, Journal of the Atmospheric Sciences, 34, 1149–1152, 1977.

ACPD

3, 1973–1989, 2003

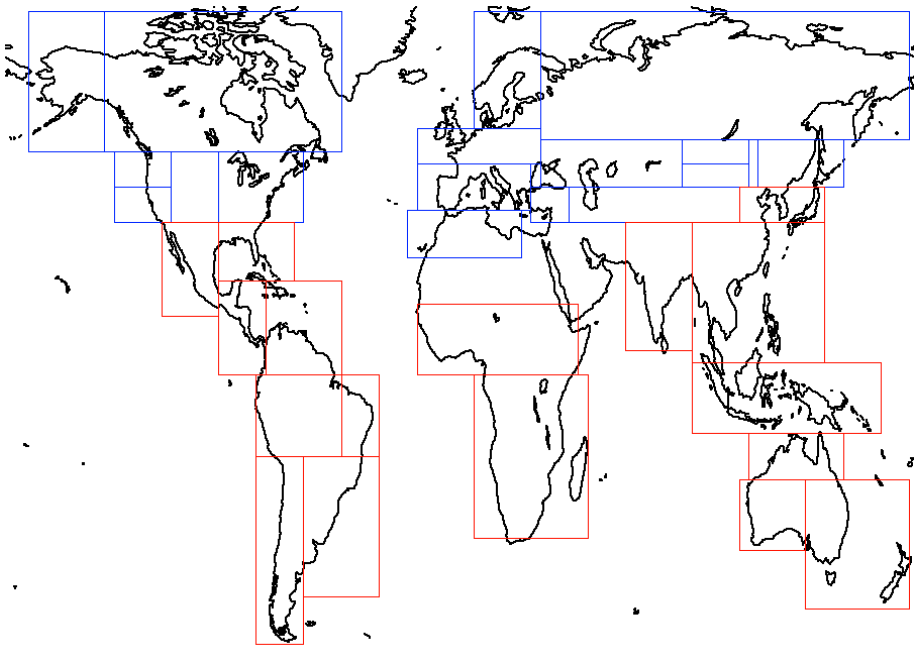

Fig. 1. Homogeneous vegetation boxes chosen to built the emission maps.

ACPD

3, 1973–1989, 2003

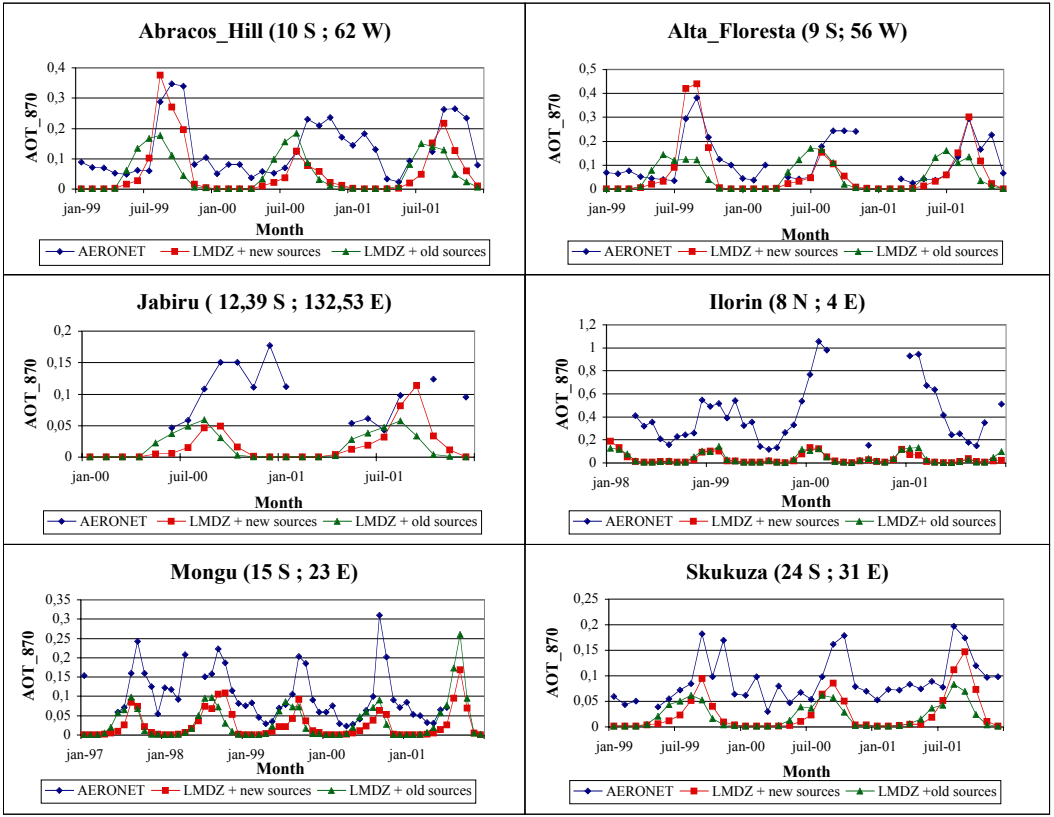

Fig. 2. AOT_{870} at different AERONET sites (blue curve) compared to LMDZ AOT_{865} with the new sources (red curve) and with the previous sources (green curve).

ACPD
3, 1973–1989, 2003

Seasonal cycle and interannual variations of biomass burning

S. Generoso et al.

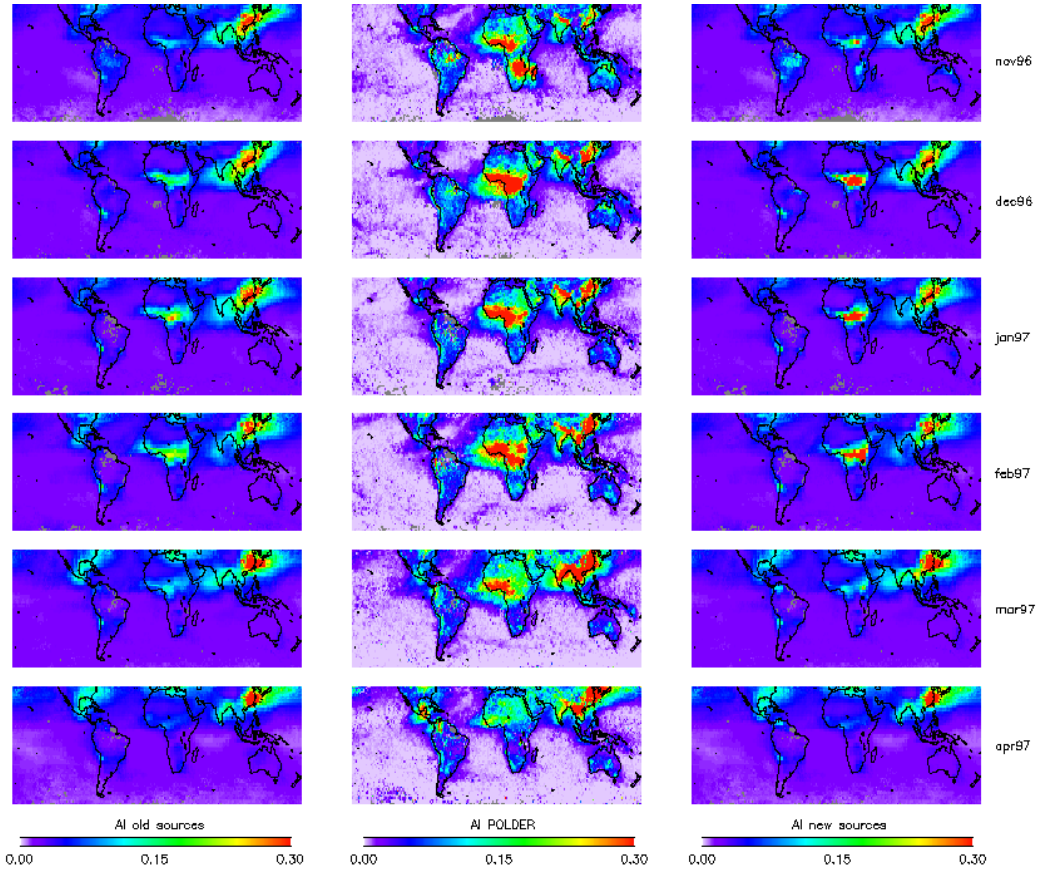

Fig. 3. (a) Comparisons between POLDER AI and LMDZ AI using both the original and the new sources from November 1996 to April 1997. LMDZ AI is obtained from AOT_{865} assuming an Angström coefficient equal to 1.5 (Dubovik et al., 2002; Liousse et al., 1995). Note that all the monthly means are computed for the days when POLDER data are available.

ACPD
3, 1973–1989, 2003

Seasonal cycle and interannual variations of biomass burning

S. Generoso et al.

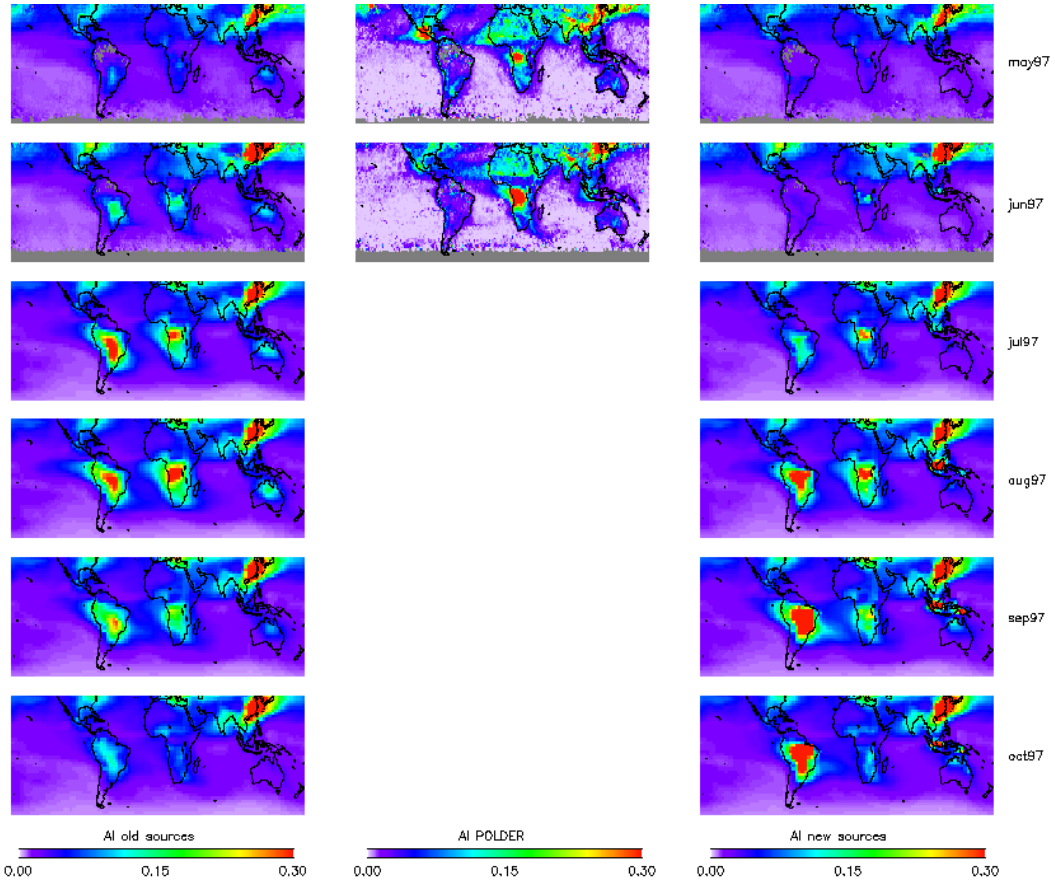

Fig. 3. (b) Comparisons between POLDER AI and LMDZ AI using both the original and the new sources from May 1997 to October 1997. LMDZ AI is obtained from AOT_{865} assuming an Angström coefficient equal to 1.5 (Dubovik et al., 2002; Liousse et al., 1995). Note that all the monthly means are computed for the days when POLDER data are available.

ACPD
3, 1973–1989, 2003

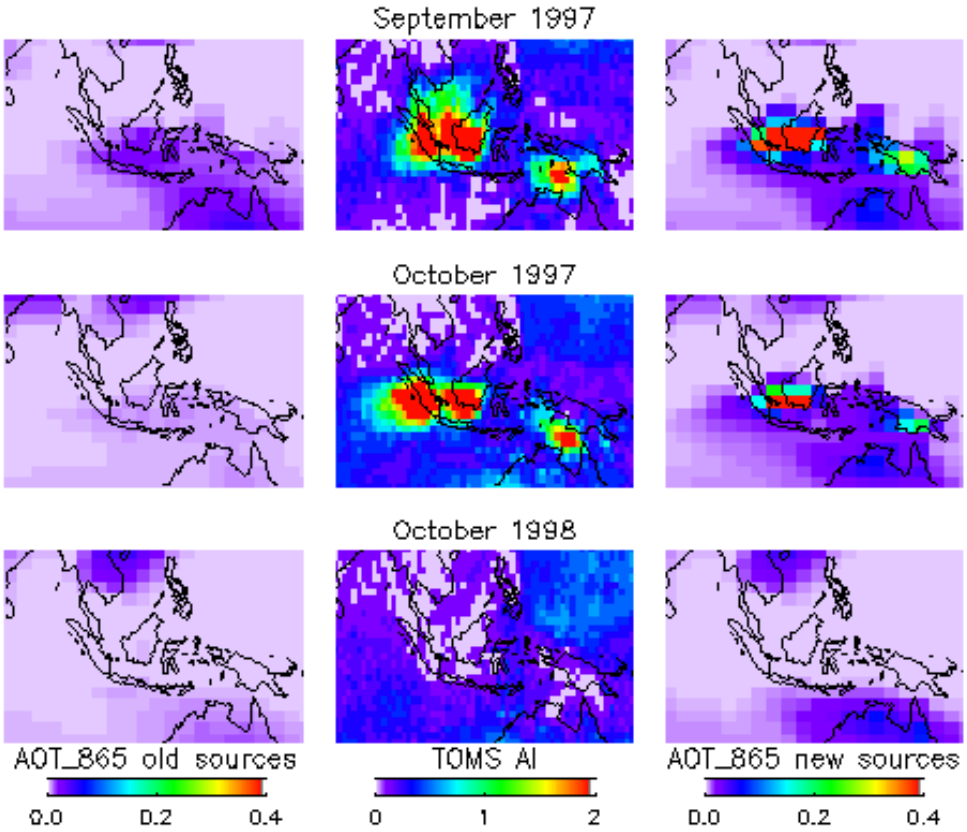

Fig. 4. Comparison of the aerosol index from the Earth-Probe TOMS (middle panels) with simulated aerosol optical depths at 865 nm simulated with (Liousse et al., 1996) inventory (left panels) and newly derived sources from ATSR fire counts (right panels). Color scales were chosen from 0 to 2 for TOMS AI and from 0 to 0.4 for LMDZ AOT in order to be consistent with the assumed value of 5 for the slope of the fit between the TOMS AI and the AOT at 865 nm based upon the Chiapello et al. (2000) study.

ACPD
3, 1973–1989, 2003